MidA is a putative methyltransferase that is required for mitochondrial complex I function

Sergio Carilla-Latorre[1], M. Esther Gallardo[1,2], Sarah J. Annesley[3], Javier Calvo-Garrido[1], Osvaldo Graña[4], Sandra L. Accari[3], Paige K. Smith[3], Alfonso Valencia[4], Rafael Garesse[1,2], Paul R. Fisher[3] and Ricardo Escalante[1,*]

[1]Instituto de Investigaciones Biomédicas "Alberto Sols" (CSIC-UAM), Arturo Duperier 4, 28029 Madrid, Spain
[2]CIBERER, ISCIII, Madrid, Spain
[3]Department of Microbiology, La Trobe University, Melbourne, Victoria 3086, Australia
[4]O. G., Bioinformatics Unit, Structural Biology and Biocomputing Program, A. V., Structural Computational Biology Group, Structural Biology and Biocomputing Program, Centro Nacional de Investigaciones Oncológicas, C/ Melchor Fernández Almagro, 3, 28029 Madrid, Spain
*Author for correspondence (rescalante@iib.uam.es)

Summary

Dictyostelium and human MidA are homologous proteins that belong to a family of proteins of unknown function called DUF185. Using yeast two-hybrid screening and pull-down experiments, we showed that both proteins interact with the mitochondrial complex I subunit NDUFS2. Consistent with this, *Dictyostelium* cells lacking MidA showed a specific defect in complex I activity, and knockdown of human MidA in HEK293T cells resulted in reduced levels of assembled complex I. These results indicate a role for MidA in complex I assembly or stability. A structural bioinformatics analysis suggested the presence of a methyltransferase domain; this was further supported by site-directed mutagenesis of specific residues from the putative catalytic site. Interestingly, this complex I deficiency in a *Dictyostelium midA⁻* mutant causes a complex phenotypic outcome, which includes phototaxis and thermotaxis defects. We found that these aspects of the phenotype are mediated by a chronic activation of AMPK, revealing a possible role of AMPK signaling in complex I cytopathology.

Key words: *Dictyostelium*, Complex I, MidA, PRO1853, *C2orf56*, LOC55471, DUF185

Introduction

Mitochondrial diseases are caused by mutations that affect genes encoded in both the mitochondrial and nuclear genomes. The pathological phenotypic outcomes of mitochondrial diseases are very complex and include blindness, deafness, epilepsy, heart disease, and muscle and neurological disorders. Although much is known about the associated mutations, the relationship between genotype and phenotype is complicated and poorly understood. Surprisingly, the same genetic defect can result in different symptoms, and conversely, similar outcomes can be caused by different genetic lesions (Debray et al., 2008; DiMauro and Schon, 2008).

Among mitochondrial diseases, deficiencies in complex I (CI) are very relevant in human pathology because about 40% of mitochondrial OXPHOS diseases involve complex I defects, and the molecular cause of this deficiency is unknown in many patients (Janssen et al., 2006; Lazarou et al., 2009). Most cellular ATP is generated by the mitochondria through aerobic respiration. Together with complex III and complex IV, CI contributes to the generation of a proton gradient across the mitochondrial inner membrane. This proton gradient is used by the ATP synthase (complex V) for ATP production. Mitochondrial CI (NADH: ubiquinone oxidoreductase, EC 1.6.5.3) is a huge multiprotein complex of 45 subunits in mammals. Of the five major respiratory complexes, CI is the least understood, partly because of its large size and complexity. Accordingly, it is believed that new components involved in the assembly, stability and/or activity of CI still remain to be identified (Koopman et al., 2010; Remacle et al., 2008).

Extensive post-translational modifications of complex I subunits have been described, most of which affect the N-termini. Examples include the loss of mitochondrial import sequences and N-alpha-acetylation. Phosphorylation in several CI subunits has also been described to affect CI function. Mutational analysis of the phosphorylation sites of NDUFA1 and NDUFB11 revealed defects in CI assembly (Koopman et al., 2010). The presence of methylation in two CI subunits has also been previously described, although the functional relevance and the methyltransferase responsible are not yet known (Carroll et al., 2005; Fearnley et al., 2007; Wu et al., 2003). In contrast to N-alpha-acetylation, which appears to be a permanent modification, and similarly to phosphorylation, protein methylation might be reversible by demethylases and might have a regulatory role.

The social amoeba *Dictyostelium discoideum* is a useful model for the study of biological issues that are relevant to human disease, including mitochondrial dysfunction (Annesley and Fisher, 2009a; Barth et al., 2007; Bokko et al., 2007; Chida et al., 2004; Kotsifas et al., 2002; Torija et al., 2006b; Williams et al., 2006). *Dictyostelium* cells feed on bacteria and remain in the form of individual cells while food is present. However, when the supply of bacteria is exhausted, starvation triggers a remarkable process of cellular chemotaxis, allowing the formation of cell aggregates. These aggregates differentiate to form phototactic migrating slugs that eventually give rise to fruiting bodies containing spores that allow *Dictyostelium* to survive (Escalante and Vicente, 2000). This developmental program is sensitive to mitochondrial dysfunction, and slug phototaxis and thermotaxis in particular are affected by diverse mitochondrial defects (Annesley and Fisher, 2009b;

Wilczynska et al., 1997). Moreover, *Dictyostelium*, as opposed to the yeast model *Saccharomyces cerevisiae*, contains all the essential CI subunits (Eichinger et al., 2005; Ogawa et al., 2000).

Traditionally, it has been assumed that mitochondrial diseases mediate their effects on the phenotype through the reduced availability of ATP. However, recent studies in *Dictyostelium* suggest that some symptoms might be the consequence of abnormal regulation of signaling pathways. The relationship between AMP-activated protein kinase (AMPK), a master regulator of the energy status of the cell, and mitochondrial diseases has been recognized recently using *Dictyostelium* as an experimental model (Bokko et al., 2007). Previous studies suggest that a chronic activation of AMPK might be a key element in some of the observed phenotypes that are present in mitochondrial dysfunction (Barth et al., 2007).

Recently, we described the identification and initial characterization of a new mitochondrial protein conserved between *Dictyostelium* and humans that we named MidA (for mitochondrial dysfunction protein A) (Torija et al., 2006a; Torija et al., 2006b). This protein belongs to an uncharacterized conserved protein family (DUF185 or COG1565). It shows high similarity to the human protein of unknown function LOC55471 encoded on chromosome 2 (C2orf56 or PRO1853).

Dictyostelium midA⁻ cells showed reduced levels of ATP and a wide array of phenotypes, including slow growth and abnormal development. In this report, we have further analyzed the function of this mitochondrial protein using an integrated approach of bioinformatics and molecular genetics in *Dictyostelium* and human cell culture. The loss of MidA generated a mitochondrial dysfunction that specifically affected CI activity and the levels of the fully assembled complex. Moreover, both *Dictyostelium* and human MidA proteins interact with NDUFS2, an essential CI core subunit. The molecular function of MidA was studied by bioinformatics and site-directed mutagenesis. The results indicate the presence in this protein family (DUF185) of a methyltransferase fold, suggesting that methylation has an important role in CI function. The phenotypic outcome observed in the *Dictyostelium midA⁻* null mutant reveals the complexity of CI mitochondrial disease and the contribution of AMPK signaling.

Results

Dictyostelium and human MidA mitochondrial proteins are required for complex I activity

Dictyostelium and human MidA are highly homologous proteins. Our previous studies in *Dictyostelium* showed that MidA is a mitochondrial protein involved in bioenergetics and its high sequence homology among species suggested the possibility of functional conservation between humans and *Dictyostelium* (Torija et al., 2006b). We wanted to test this hypothesis and extend our knowledge of the function of these proteins. Consequently, our first aim was to determine the subcellular localization of MidA in human cells. A construct expressing the human protein fused to GFP was transiently transfected into HeLa and HEK293T cells, which were then stained with the mitochondria-specific dye Mitotracker Red. As shown in supplementary material Fig. S1, human MidA was also localized in mitochondria.

We next took advantage of comparative genomic tools to design working hypotheses about MidA function. There are homologues of MidA in many organisms but it seems to be absent in others and this phylogenetic profile might provide important functional clues. It is expected that proteins working together in a given function will have the same phylogenetic profile. Using the String server

(http://string.embl.de/), we obtained very similar phylogenetic profiles for CI subunits, well known CI assembly factors and MidA. A more detailed analysis using a wide array of species is shown in supplementary material Table S1. There is a clear correlation between the presence of MidA and a representative complex I subunit (NDUFS7). It is well known that CI is not present in all eukaryotes (such as fermentative yeasts *S. cerevisiae* and *S. pombe*) but it is present in higher eukaryotes and *Dictyostelium* where it has a key role in ATP generation. As expected, MidA has no homologues in *S. cerevisiae* and *S. pombe*. Interestingly, MidA homologues are also found in α-proteobacteria, the closest living organisms to the putative precursors of eukaryote mitochondria.

To test the hypothesis of a functional connection between MidA and CI, we measured the activity of the OXPHOS complexes (I, II, III and IV) in *Dictyostelium midA⁻* null cells. A 50% decrease in the activity of CI in *Dictyostelium* was observed (Fig. 1A). Interestingly, the activity of the other complexes was either unaffected or was significantly higher in the mutant. This might be explained by a compensatory response to the loss of CI activity.
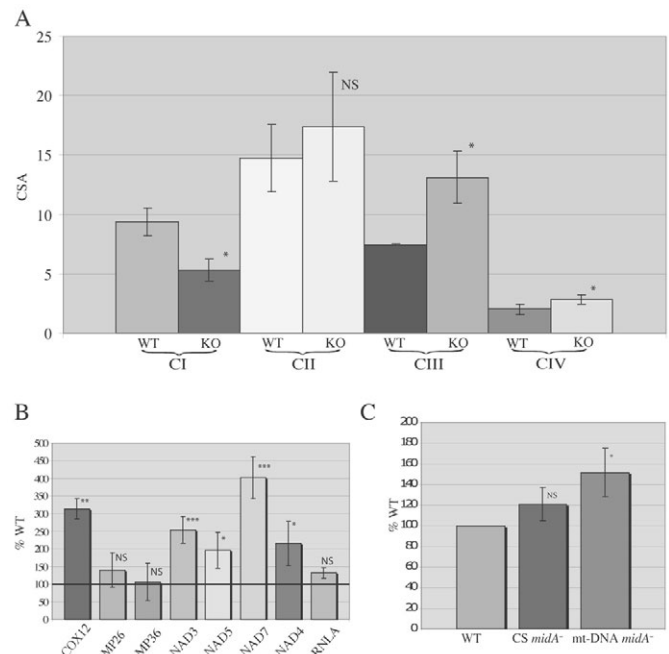

Fig. 1. The activity of complex I is reduced in cells lacking MidA.
(**A**) Spectrophotometric analysis of the activity of complexes I, II, III and IV in *Dictyostelium* WT and *midA⁻* mutant cells. At least three independent experiments for each complex were performed and the bars represent mean ± s.d. Significance of differences were determined by Student's *t*-test; *$P<0.05$; **$P<0.01$; ***$P<0.001$; n.s., non-significant difference. Reduced activities of complex I were observed in *midA⁻ Dictyostelium* cells. CSA, complex specific activity, corrected by citrate synthase. (**B**) The steady-state levels of expression of representative genes from the eight major polycistronic transcripts from mitochondrial RNA were measured and compared with the levels found in wild-type control cells. Five of them showed significant increases compared with wild-type cells. Three independent experiments were performed and the bars represent the mean ± s.d. Significance of differences were determined by Student's *t*-test and indicated by the *P* value, as described above. (**C**) The level of the activity of the mitochondrial enzyme citrate synthase (CS) and amount of mtDNA was measured and compared with the wild type (adjusted to 100%). Three independent experiments were performed and the statistical analysis was carried out as described above.

Consistent with this possible compensatory response, increases were also observed in the mutant in the steady state levels of mtDNA and most mtRNA transcripts (Fig. 1B,C). There also appeared to be a small, albeit statistically insignificant, increase in the activity of citrate synthase (Fig. 1C).

The level of assembled complex I is reduced in HEK293T cells where MidA is downregulated

We next wanted to study the level of assembled complex I by blue native (BN)-PAGE. We were unable to use *Dictyostelium* cells in these analyses owing to the lack of available antibodies to detect the different complexes and the low signal obtained by BN-PAGE. Therefore we used stable transfectants of HEK293T cells in which human MidA was downregulated by shRNAmir technology. Two different clones (S1 and S19) were obtained with a level of *MidA* mRNA downregulation of 93% and 87%, respectively. A control clone transformed with a scrambled vector showed no reduction in *MidA* mRNA. Fig. 2A shows representative gels and Fig. 2B a quantification by densitometry of three independent experiments where the level of CI had been normalized using the signal of complex III. Similar results were obtained when we normalized for complex II, complex IV and complex V (data not shown). We found a modest effect in fully assembled CI that ranged from 60% to 80% with respect to the control, which was treated with

Fig. 2. Reduction of fully assembled complex I in human cells with downregulated MidA. (**A**) Mitochondrial complexes from human HEK293T clones S1 and S19, and control cells were extracted with N-dodecyl β-D-maltoside for BN-PAGE analysis. The gel was transferred to PVDF membrane and incubated with a cocktail of antibodies for complex detection. The different bands were assigned by the expected pattern and their approximate size calculated using a protein size standard. A significant reduction in CI levels (indicated by rectangle) was observed. (**B**) Densitometric quantification of three different BN-PAGE western blots showed a reduction of assembled CI to approximately 70-80% of that found in a clone harboring a scrambled vector. Densitometry was performed with ImageJ 1.33u (NIH, USA), and the values for CI were normalized to those of complex III. The bars represent mean ± s.d. $P=0.060$ for S1 and $P=0.033$ for S19 (Student's *t*-test).

scrambled shRNA. The activity of CI was also measured by spectrophotometric analysis. A reduction in CI activity was only detected in clone S1, which had higher levels of mRNA inhibition. This clone showed an average CI activity that was 75% of that in control cells (data not shown). Together, these results suggest that both *Dictyostelium* and human MidA are involved in complex I assembly or stability.

MidA interacts with complex I subunit NDUFS2

In a parallel approach to elucidate the function of MidA, we performed a yeast two-hybrid screening to identify possible interactors. As bait we used the whole *Dictyostelium* MidA protein, except for the first 21 amino acids, which correspond to the putative mitochondrial targeting sequence. The vector used was pB29, which contains an N-bait-LexA-C fusion, and 57.4 million interactions were analyzed. Interestingly, ten independent positive clones were obtained that encode *Dictyostelium* NADH-ubiquinone oxidoreductase-chain 49 (DDB_G0294030), a homologue of the human complex I subunit NDUFS2. Fig. 3A shows the common region contained in the different clones that allowed us to restrain the minimal interaction region to 40 amino acids. This interaction was ranked with high confidence by a computer program (Global PBS®, Predicted Biological Score from Hybrigenics) that represents the probability of an interaction to be non-specific (Rain et al., 2001). Nevertheless, a further validation was performed using pull-down assays. The N-terminal fragment of *Dictyostelium* NDUFS2, which contains the minimal region of interaction, was fused to GST, purified from bacteria and incubated with cell extracts from *Dictyostelium* expressing MidA fused with GFP. As shown in Fig. 3B, MidA-GFP was pulled down by GST-NDUFS2 but not by GST alone, which was used as a control. We also wanted to validate this interaction using human MidA, expressed in HEK293T cells fused with GFP. The bacterially expressed N-terminus of human NDUFS2 was used in the assay (Fig. 3B). A positive pull-down was observed, again suggesting a functional conservation between *Dictyostelium* and human MidA proteins.

We next asked whether the observed interaction requires the functional methyltransferase domain identified in the MidA sequence (see below). We performed pull-down assays using *Dictyostelium* cell extracts expressing wild-type and mutated MidA (G170V) in which the methyltransferase domain is presumed to be inactivated (see below). As shown in Fig. 3C, both proteins were pulled down by the bacterially expressed *Dictyostelium* NDUFS2, suggesting that a functional methyltransferase domain is not required for the interaction.

Is MidA stably bound to CI or any other large subcomplex? To answer this question, we used the same *Dictyostelium* rescued strain used in the pull-down experiments that stably expressed MidA-GFP to perform a second-dimension analysis. After BN-PAGE, the lane was cut and resolved in a second SDS-denaturing dimension and MidA-GFP was detected by western blot analysis (supplementary material Fig. 2B). MidA had an apparent molecular size in the first dimension that was compatible with it being a homodimer (approximately 200 kDa, after taking into account the size of the GFP and TAP tags). Although most of the MidA protein is present as a dimer, a signal was also detected at higher molecular sizes (ranging from 450 to 750 kDa) (supplementary material Fig. S2B). *Dictyostelium* CI has an approximate molecular weight of 880 kDa, as determined previously by MALDI-TOF analysis of the corresponding band from BN-PAGE gels (supplementary material Fig. S2A). Therefore, *Dictyostelium* MidA does not seem
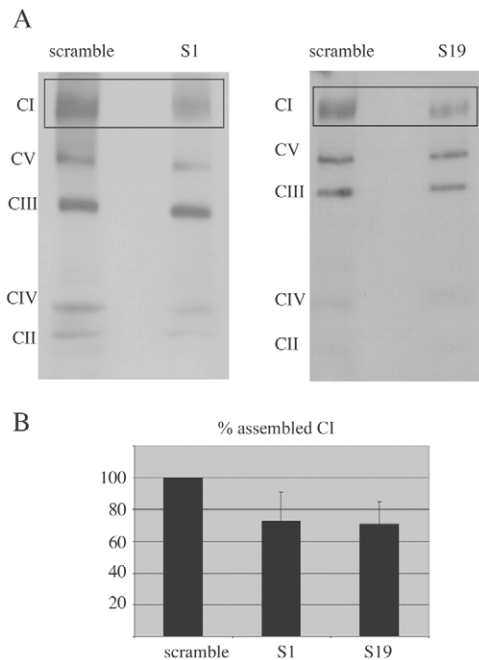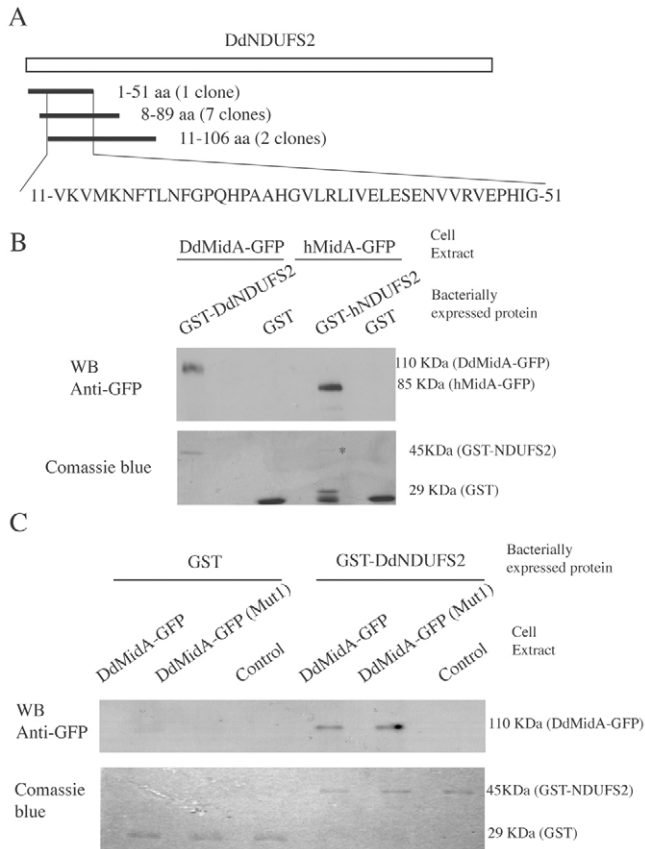
Fig. 3. MidA interacts with NDUFS2. (**A**) A yeast two-hybrid screening using *Dictyostelium* MidA as bait rendered a possible interaction with the N-terminus of the complex I core subunit NDUFS2. The open rectangle represents the complete amino acid sequence of *Dictyostelium* NDUFS2 and the lines below mark the position and the number of the different clones that gave a positive interaction in the screening. The amino acid sequence of the overlapping minimal region is also shown. (**B**) The interaction was validated by pull-down assay using bacterially expressed NDUFS2 fused with GST and cell extracts expressing *Dictyostelium* MidA and human MidA fused to GFP. A fraction of the bacterially expressed proteins used in the assay are shown by Coomassie blue staining after SDS-PAGE electrophoresis. Human NDUFS2 was sensitive to degradation and little protein was obtained (labeled with an asterisk). After incubation with the indicated cell extracts and subsequent washes, the samples were separated by SDS-PAGE, transferred and incubated with anti-GFP antibody. Both *Dictyostelium* and human MidA-GFP were efficiently pulled down and showed the expected molecular size. (**C**) Similar pull-down assays were performed using *Dictyostelium* cell extracts expressing MidA-GFP as before, or a mutated form (G170V), indicated as MidA-GFP (Mut1). A wild-type extract was used as an additional negative control. The lower blot shows the bacterially expressed proteins used in the assay stained with Coomassie blue. The upper blot shows both proteins interacting with NDUFS2.

to be stably bound to CI, but might be present in high molecular mass CI subcomplexes. This is in agreement with previous proteomic studies that have not detected MidA as part of CI (Fearnley et al., 2007). A similar experiment was performed with HEK293T expressing human MidA-GFP and we found no stable association of the human protein with subcomplexes, although its size suggested that it is also a homodimer (data not shown). Perhaps the interaction of the *Dictyostelium* protein in large complexes is more stable than that of the human homologue, allowing its

detection by this technique, or there might be functional differences between species that we do not yet understand.

MidA has a conserved methyltransferase fold

The lack of obvious functional motifs in MidA amino acid sequences prevented us from speculating about the possible molecular function (Torija et al., 2006b). We have now searched for structural similarities with other proteins whose function is known and carried out bioinformatics modeling. To obtain a structural model for MidA, we performed an initial Blast search against PDB, the database of protein structures, to find a homologous protein of known structure (Altschul et al., 1997; Kirchmair et al., 2008). We found a highly similar candidate with 32% sequence identity with MidA and a Blast E-value of 2e-52. This protein belongs to *Rhodopseudomonas palustris* and is a target of a structural genomics consortium (Uniprot code Q6N1P6, PDB code: 1zkd). Its function is still unknown, as shown by its placement in the PFAM database of conserved domains as a DUF185 member, a family of proteins of unknown function (Finn et al., 2008). However, in the SCOP database of the structural classification of proteins (Andreeva et al., 2008), 1zkd was classified as a possible member of the S-adenosyl-L-methionine (SAM)-dependent methyltransferases, a large superfamily of proteins that is comprised of 52 protein families.

Using 1zkd as a template, a 3D model of MidA was built using the Phyre server (Kelley and Sternberg, 2009). From the set of models returned by this server, the one at the top of the list uses 1zkd as template, reflecting once more the relatedness of the two proteins. The sequence-to-structure alignment between MidA and 1zkd covered most of the MidA sequence (Fig. 4A). Of course, the MidA N-terminal sequence corresponding to the putative mitochondrial-targeting peptide, is totally excluded in the model.

We next wanted to define the functional residues that might occur in the catalytic site using FireStar (Lopez et al., 2007), a web server that predicts functionally important residues using FireDB (Lopez et al., 2007). FireDB is a database of PDB structures and their associated ligands, and contains the largest set of reliably annotated functionally important residues. These annotations are extracted from protein-ligand atom contacts and are also derived from the catalytic-site atlas (CSA) (Porter et al., 2004). Interestingly, the information obtained from FireStar indicated a relationship between the sequence of MidA and a human dimethyladenosine transferase (PDB code 1zq9, chain A). Following the FireStar annotations derived from the CSA, the catalytic site of 1zq9 contains three relevant residues: G64, E85 and N128. The two first are conserved in MidA (G170 and E200), whereas the third is replaced by a glutamine (Q257). The structure of the human dimethyladenosine transferase (1zq9) is available (PDB code 1zq9, chain A) and 1zq9 was crystallized with S-adenosylmethionine (SAM), the methyl donor, that was in contact with these three residues. We superimposed our MidA 3D model with the region that contains the 1zq9 catalytic site (residues 64-128) using local-global alignment (LGA) (Zemla, 2003), and found that they superimposed fairly well, as shown in Fig. 4B.

To determine whether the SAM ligand can be accommodated in our MidA model in the proper manner, a docking was performed using the Haddock biomolecular docking software by searching 1000 models. The only spatial restriction imposed on Haddock was to keep SAM close to the equivalent three residues in our model. We obtained several clusters of models, and finally selected the first ten models of the best cluster. These models had good
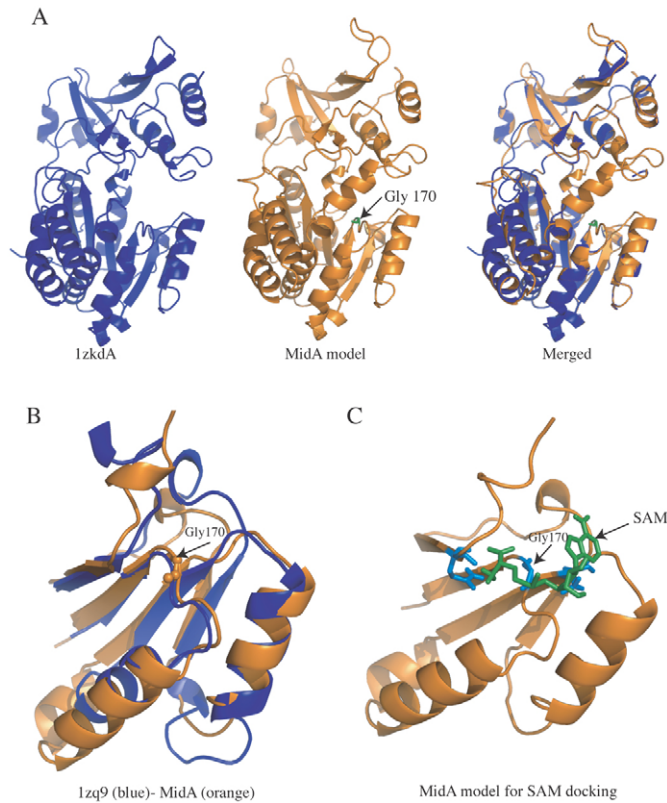
Fig. 4. MidA contains a methyltransferase domain. (**A**) A 3D model of MidA was built using as a template 1zkd, a *Rhodopseudomonas palustris* protein that belongs to DUF185 family. The blue diagram represents 1zkd, chain A from PDB (this protein is a homodimer and chain B is not displayed). The orange diagram shows the MidA model. The structural alignment between MidA and 1zkd is shown on the right and covers most of the MidA sequence. (**B**) Detail of the alignment of the MidA model and 1zq9. The catalytic region of the 3D model of MidA (orange) superimposes fairly well with that of 1zq9 (blue), a human dimethyladenosine transferase whose structure is known, showing a characteristic fold exposing a loop where several conserved residues reside. Among them, Gly170, was chosen for functional analysis. (**C**) The methyl donor SAM fits in the MidA model. Docking was performed running Haddock. SAM maintains the correct distances to the equivalent critical residues of the methyltransferase 1zq9. Residues G170, E200 and Q257 are blue and SAM is colored in green.

Haddock scores and were very similar, with a maximum interface ligand RMSD of 1.5 Å. The first ranked model is shown in Fig. 4C. The network of contacts between MidA and SAM remained, as shown with Ligplot (Wallace et al., 1995) in supplementary material Fig. S3, keeping the three aforementioned residues in contact with SAM.

The next step was to simulate the effect of the mutation G170V. We first replaced G170 with a valine with PyMol over the docking model (The PyMol Molecular Graphics System, DeLano Scientific, Palo Alto, CA) by selecting the rotamer that appears to be more frequent in proteins. Obviously, the effect of this mutation produced new clashes and so required a new docking of SAM with respect to the mutated model. We ran Haddock again to better accommodate the SAM molecule. Once more, we picked the first ten models of the best cluster, and checked the level of conservation of the spatial distance with respect to the three aforementioned residues in the

mutation model. The new docking model allowed us to determine that the initial network of contacts was lost, and that SAM was now accommodated towards the exterior of the protein, presumably causing a loss of the function of the enzyme. This was confirmed experimentally by site-directed mutagenesis, as described below.

The crystal structure of 1zq9 indicates that the protein is homodimeric, as described for other methyltransferases. It should be noted that the BN- and SDS-PAGE analysis described above suggested that MidA is also a dimer (supplementary material Fig. S2).

The methyltransferase domain is required for MidA function

The structural model shown above strongly suggested the presence of a SAM-binding motif, which is characteristic of methyltransferases. To confirm this hypothesis, we performed site-directed mutagenesis to change residue G170, which is present in the conserved folding and whose change to valine was predicted to have a deleterious effect on the binding of SAM. A double mutation was also performed to change both G170 and G172 to valines. Both residues have been previously suggested to be important for SAM binding, and are well conserved among methyltransferases (Niewmierzycka and Clarke, 1999). The WT and mutated forms of MidA were fused to GFP to monitor their expression and localization in the cells and transformed into the *Dictyostelium midA⁻* null mutant (Fig. 5A). As described previously, *midA⁻* cells show defects in growth both in axenic medium and in association with bacteria, as a consequence of the mitochondrial dysfunction (Torija et al., 2006b). Although the WT protein complemented the phenotype completely, the G170 mutated protein was not able to complement the phenotype (Fig. 5C). A similar result was obtained for the G170 and G172 double mutation (data not shown). To exclude the possibility that the lack of complementation was a result of failed targeting to the mitochondria, we checked and showed that the proteins were localized in the mitochondria (Fig. 5B shows the result for the G170V mutant as an example). The lack of reversion of the phenotype strongly suggests that a single mutation in G170 from the methyltransferase domain is sufficient to render the protein inactive. These results also suggest that the putative methyltransferase domain is required for MidA function in *Dictyostelium*.

Characterization of MidA complex I deficiency and its relationship with AMPK signaling

To gain a better understanding of the genotype-phenotype relationship in mitochondrial dysfunction, we made use of *Dictyostelium* cells lacking MidA (*midA⁻* null mutant) as a cellular model for CI disease. We wanted to characterize in detail the phenotype of the null mutant and to study the relationship with AMPK signaling. *Dictyostelium* cells aggregate upon starvation to form a multicellular organism. At the slug stage, these structures show a remarkable capacity to move towards light and thermal gradients. This phototaxis and thermotaxis ability was shown to be more sensitive to mitochondrial dysfunction than other cellular functions (Kotsifas et al., 2002; Wilczynska et al., 1997). The *midA⁻* mutant showed a strong defect in phototaxis, as observed by the slug-trail assay (Fig. 6A, upper panel) and quantification of the accuracy of phototaxis (κ) (Fig. 6A, lower panel). κ measures how concentrated the trails are around the direction of the light source. It ranges from 0 when there is no orientation in any preferential
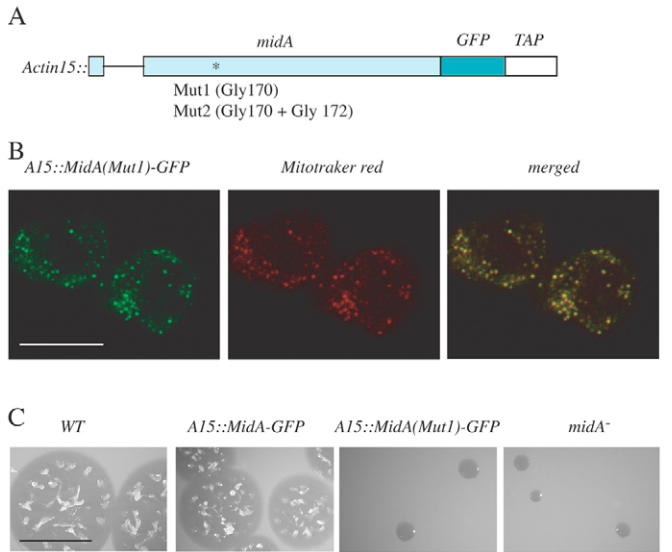
Fig. 5. Site-directed mutagenesis supports the presence of a methyltransferase domain. (**A**) Scheme of the expression constructs used for complementation studies. The coding region of the *midA* gene, fused to GFP and TAP (tandem affinity purification tag), is directed by the Actin15 (A15) promoter and is depicted as open boxes. A thin line represents an intron near the N-terminus. Site-directed mutagenesis was performed at the indicated residues (asterisk). (**B**) The wild-type and mutated constructs were transformed in the *midA⁻* mutant and stable transformant clones were checked for expression and localization of MidA in mitochondria. All the constructs showed mitochondrial localization of the protein. A representative analysis is shown for the mutated construct (G170V). Colocalization was observed between MidA-GFP (green) and mitotracker (red), indicating mitochondrial localization. Scale bar: 10 µm. (**C**) Analysis of growth in association with bacteria of transformant clones with WT and the mutated forms of MidA. The WT construct complemented the growth phenotype and other aspects of the phenotype (not shown). However, the constructs containing the indicated mutations were not able to complement the phenotype, giving rise to the small colony phenotype that is characteristic of *midA⁻* mutant. A representative analysis is shown for the mutation G170V. Scale bar: 1 cm.

direction to infinity in the case of a perfect orientation. The defect in phototaxis was restored in a *midA⁻* mutant strain where *Dictyostelium* MidA had been transformed with an expression vector under the control of an actin promoter (rescued strain). Similarly, a defect in thermotaxis was also observed, as shown in Fig. 6B where κ was measured in the wild type, the *midA⁻* mutant strain and the rescued strain during thermotaxis at different temperatures (Fig. 6B). Thermotaxis was also complemented in the rescued strain. Additionally, *midA⁻* mutants showed a growth defect that is accompanied by a phagocytosis and macropinocytosis defect, as previously described (Torija et al., 2006b) and shown in supplementary material Fig. S6. These defects in phagocytosis and macropinocytosis have not been observed previously in other mitochondrial *Dictyostelium* mutants, suggesting a more complex scenario, which will be discussed below (Barth et al., 2007).

We next explored the contribution of AMPK signaling in the complex phenotype of *midA⁻* cells. Overexpression of an AMPK antisense construct has been previously shown to inhibit the expression of AMPK and to restore phototaxis in several *Dictyostelium* mutants. As expected, we found that phototaxis and partly thermotaxis were restored in the *midA⁻* mutant when AMPK was downregulated suggesting that this phenotype is mediated by
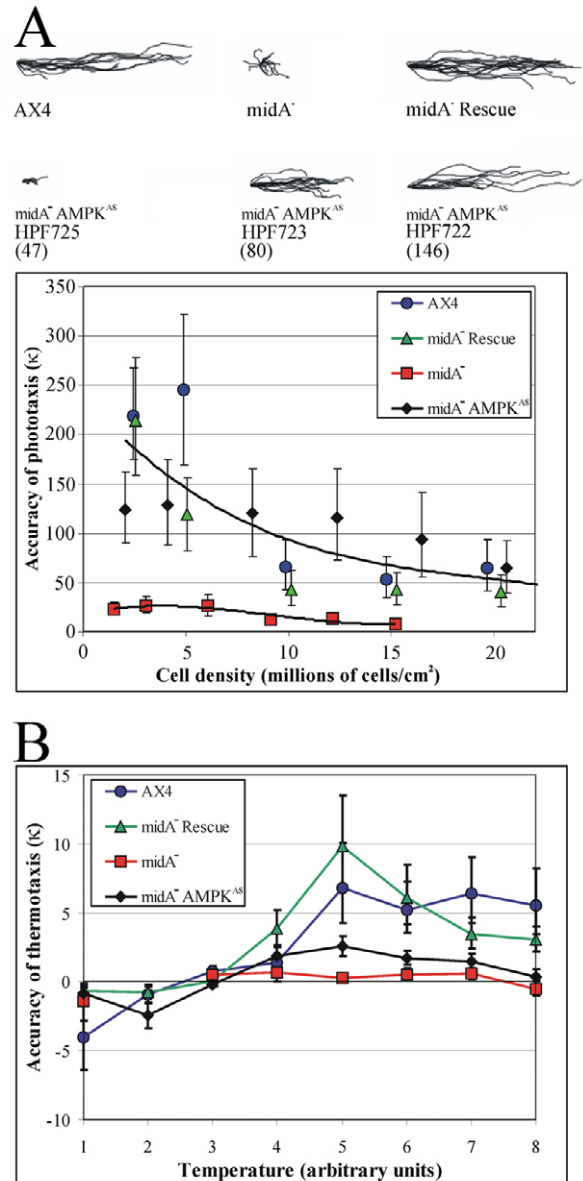

Fig. 6. Phototaxis defects in *Dictyostelium* MidA mutant can be rescued by AMPK inhibition. (**A**) Different *Dictyostelium* strains were allowed to form migrating slugs and exposed to lateral light to determine their phototaxis capabilities. The strains used were the following: wild-type *Dictyostelium* cells (AX4), the *midA*-null mutant (*midA⁻*), a complemented strain ectopically expressing the complete *midA* gene (*midA⁻* Rescue) and several independent transformants (strain designations beginning with HPF) of the MidA mutant expressing different numbers of copies of an AMPK antisense construct (*midA⁻* AMPK^{AS}). The copy number for the AMPK antisense construct (pPROF362) is indicated within brackets. The phototaxis and migration (short trails) defects of the *midA⁻* mutant were suppressed in a copy number-dependent manner. In the lower panel, the accuracy of phototaxis (κ) was measured for the indicated strains at different cell densities. In this experiment, the *midA⁻* AMPK^{AS} strain was HPF722. (**B**) Defective thermotaxis in the *midA⁻* mutant is complemented by ectopic expression of MidA and suppressed by AMPK antisense inhibition. The accuracy of thermotaxis in a 0.2°C/cm gradient was measured for slugs formed at a density of 3×10^6 cells/cm^2 and migrating at temperatures ranging from 1 to 8 (arbitrary units corresponding in separate calibration experiments to 14°C to 28°C). The *midA⁻* AMPK^{AS} strain was HPF723 and it exhibited substantial (but not complete) suppression of the thermotaxis defect. Other details are as for A.

a chronic activation of the kinase (Fig. 6A). This is the first report that a phenotypic defect caused by a specific CI deficiency in a model system can be rescued by AMPK downregulation. Interestingly, the defects in growth, phagocytosis and macropinocytosis were not rescued by the same experimental manipulation, suggesting that these defects are independent of AMPK signaling in the *midA⁻* mutant (supplementary material Fig. S4).

Discussion

We used bioinformatics and experimental comparative analysis in *Dictyostelium* and human cells to shed light on the function of MidA, a protein that is conserved from bacteria to humans and contains a characteristic DUF185 motif of unknown function. The functional similarities between *Dictyostelium* MidA and its human homologue strongly suggest that both proteins are orthologous proteins that contain a methyltransferase domain and required for mitochondrial CI function. Another putative methyltransferase has recently been described to function in CI assembly or stability (Gerards et al., 2009; Sugiana et al., 2008), highlighting the potentially important but poorly understood role of methylation in CI function.

About 40% of inherited disorders of the OXPHOS system involve isolated or combined deficiencies in CI, the largest complex of the OXPHOS system. The genetic cause of many cases of CI deficiencies is still unknown, which is due in part to insufficient understanding of the CI assembly process and the factors involved. We do not know yet whether MidA is involved in human mitochondrial disorders, but it should definitely be considered a strong candidate. The loss of function of this protein in the model *Dictyostelium* generates a complex phenotypic outcome, including growth and developmental defects. In humans, disorders associated with CI dysfunction are also complex, and usually lead to multisystem failure that affects the brain, skeletal muscle and heart.

Dictyostelium midA⁻ null cells showed a decreased activity of CI, and BN-PAGE studies in human cells where MidA is downregulated also showed lower amounts of fully assembled complex, suggesting a role for MidA as an assembly or stability factor. The level of the assembly and activity of human CI in the knockdown cells was around 70% of the control values, a moderate effect but near the threshold that could have an impact in cellular bioenergetics (Pathak and Davey, 2008), or even cause human disease (Loeffen et al., 2001). CI is formed by a large number of subunits (up to 45 subunits in humans). The assembly and stability of such a large multiprotein complex requires specific chaperone and assembly factors, six of which have been implicated in human CI deficiency, including NDUFAF1-NDUFAF4 (Hoefs et al., 2009; Ogilvie et al., 2005; Saada et al., 2009; Vogel et al., 2005), C8ORF38 (Pagliarini et al., 2008) and C20ORF7 (Gerards et al., 2009; Sugiana et al., 2008). Others such as Ecsit (Vogel et al., 2007), AIF (Vahsen et al., 2004) and IndI (Bych et al., 2008) are required for CI assembly, but have not yet been implicated in human disease.

In spite of its large size, CI has a basic catalytic core formed by only 14 proteins that are evolutionarily conserved from prokaryotes to humans. All have been implicated in human CI disorders, including NDUFS2 (Loeffen et al., 2001; Ugalde et al., 2004), an iron-sulfur protein that we have shown to interact with MidA/PRO1853. NDUFS2 is encoded by the nuclear genome of human cells but it is encoded by the mitochondrial genome in *Dictyostelium* revealing its ancient origin as an endosymbiont

protein. Interestingly, MidA homologues also exist in α-proteobacteria, suggesting that the interplay between MidA protein and the catalytic CI is of ancient origin and conserved from bacteria to humans.

The SAM-dependent methyltransferase enzymes share little sequence identity, but do contain a highly conserved structural fold that is involved in SAM binding. Surprisingly, the precise residues that bind the SAM cofactor are poorly conserved (Loenen, 2006; Schubert et al., 2003). We have shown by bioinformatics modeling and site-directed mutagenesis that DUF185 might have a methyltransferase domain. At the level of amino acid sequence, only a short region of homology can be detected between DUF185 proteins and methyltranferases, the so-called motif I, corresponding to a loop of the catalytic core involved in SAM binding (Niewmierzycka and Clarke, 1999). The consensus sequence was defined as a nine-residue block, hh(D/E)hGxGxG, where h represents a hydrophobic residue and x can be any residue (Kakebeeke et al., 1979; Niewmierzycka and Clarke, 1999). In previous studies based on multiple protein alignments, this short sequence was revealed and led to the proposal that DUF185 is a methyltransferase (Sadreyev et al., 2003). Our site-directed mutagenesis studies targeted the first two conserved glycines present in this sequence and showed that the first and possibly both of these residues are required for the protein function. Five different structural folds have been described to bind SAM and perform a methyl transfer. Our model fits with class I, the most abundant, which is composed of alternating β-strands and α-helices (Martin and McMillan, 2002; Schubert et al., 2003). Taken together, these studies strongly suggest that MidA proteins contain a methyltransferase domain. The characterization of its biochemical activity and the identification of the possible targets are of great interest and will warrant further investigation.

Methyltranferases are a large family of proteins that are involved in methylation of a wide variety of substrates including DNA, RNA and proteins and the atomic targets can be carbon, oxygen, nitrogen and sulfur. However, in most cases, no specific traits in the sequence or the structure can be reliably used to predict the substrate of the modification. Indeed, motif I is present in DNA, RNA, protein and small molecule methyltransferases (Kagan and Clarke, 1994). In mitochondria, methylation has an essential role. Mitochondrial DNA, tRNA and rRNA are all targets of specific methylation events (Helm et al., 1998; Pintard et al., 2002) and specific carriers transport SAM into the mitochondria (Agrimi et al., 2004). As far as protein methylation is concerned, only two methylated subunits have been detected in complex I subunits. One of them is the bovine NDUFB3 (B12), which is methylated at conserved His residues. Interestingly, the other one is the human NDUFS2, which harbors a methylated arginine, R323. Of course, the interaction of MidA with NDUFS2 and subsequent methylation of the subunit is an attractive hypothesis that remains to be investigated. The possible functional relevance of NDUFS2 methylation is not known but it is likely that this post-translational modification in such an important core subunit alters the assembly or the stability of the whole complex. In fact mutations in Arg228, Ser413 and Pro229 of NDUFS2 have been described to be involved in CI disease (Loeffen et al., 2001). However, we should also consider the possibility that MidA has a dual function as a chaperone and as a methyltransferase. MidA is not stably bound to CI, as suggested by our results using BN-PAGE. Therefore, it is possible that the interaction with NDUFS2 occurs during the assembly process of

the complex, thus functioning as a transitory step that is required for correct CI stability.

The complex phenotypes of *Dictyostelium* cells deficient in MidA show similarities with other strains with mitochondrial disease, but there are also differences. Defects in phototaxis and thermotaxis have been described previously in other *Dictyostelium* mitochondrial dysfunctions that affect respiration, such as ethidium-bromide-mediated mtDNA depletion and the antisense inhibition of Chaperonin 60 (Cpn60) (Bokko et al., 2007; Chida et al., 2004; Kotsifas et al., 2002; Wilczynska et al., 1997). Interestingly, the phototaxis impairment in the MidA mutant can be rescued by AMPK inhibition, similarly to the other described mitochondrial mutants. However, *midA⁻* cells showed a severe defect in phagocytosis and macropinocytosis: a phenotype that is not rescued by AMPK antisense inhibition and is not even present in the other described mitochondrial mutants. This defect would, in turn, explain the AMPK-independent impairment of growth that we observe in the MidA-null mutant. The results suggest that either MidA itself or CI activity are specifically required for normal phagocytosis and pinocytosis.

We observed compensatory responses that increased the expression and level of activity of other respiratory chain complexes and the amount of mtDNA in the cells. This suggests a feedback that stimulates mitochondrial biogenesis and ATP production, but fails to correct the specific CI deficiency caused by the absence of MidA. AMPK might participate in this feedback, because it stimulates mitochondrial biogenesis and ATP production in *Dictyostelium*, as in other organisms (Bokko et al., 2007). The pattern of phenotypic outcomes in the MidA-null mutant thus results from both chronic AMPK activity and a specific failure of the associated feedbacks to correct the CI deficiency. This reveals once more the complexity of mitochondrial cytopathology and specifically in CI diseases. The observation of the role played by AMPK signaling in complex I pathology in *Dictyostelium* suggests that in humans some of the associated phenotypes might also be mediated by chronic activation of this signaling pathway. If so, treatment aimed to regulate AMPK signaling might be beneficial.

Materials and Methods

Dictyostelium growth, transformation and development
Dictyostelium AX4 cells were grown axenically in HL-5 medium or in association with *Klebsiella aerogenes* in SM plates (Sussman, 1987). Transformations were carried out by electroporation, as described previously (Pang et al., 1999). For synchronous development, axenically growing cells were washed from culture medium by centrifugation, resuspended in water or PDF buffer and deposited on nitrocellulose filters (Shaulsky and Loomis, 1993).

Human cell culture and RNA interference
HEK293T and HeLa cell lines were obtained from the American Type Culture Collection (ATCC) (Manassas, VA) and were grown following the specifications of the repository. Two different micro RNA adapted short-hairpin RNAs (shRNAmir) cloned into pGIPZ vector (V2HLS_31857 and V2HLS_31862; Open Biosystems) were used to stably knockdown the human gene encoding MidA (*C2orf56*). Lipofectamine 2000 (Invitrogen) was used for transfection of the constructs according to the manufacturer's protocol. For selecting stable cell lines, the puromycin drug-resistance marker was used. Relative quantitative real-time PCR was carried out to estimate the knockdown levels of the human gene in a 7900HT Fast Real Time PCR system (Applied Biosystems). For this purpose, two different TaqMan assays were used. One specifically detected the levels of mRNA encoding MidA (Hs00218600; Applied Biosystems). The other was a TaqMan ribosomal RNA control designed to detect the 18S ribosomal RNA gene as endogenous control (4308329; Applied Biosystems).

Mitochondrial localization
Mitochondrial localization with Mitotracker Red (Molecular Probes) was performed as previously described (Torija et al., 2006b). Confocal analysis was performed in a

Leica TCS SP5 using a PL APO 63×/1.4-0.6 objective and LAS-AF (Leica Application Suite) software.

Spectrophotometric analysis of the OXPHOS complexes and BN-PAGE
For spectrophotometric analysis, 5×10^7 growing cells were centrifuged and washed once with PBS. The pellet was resuspended in 2 ml SETH buffer (250 mM sucrose, 2 mM EDTA, 10 mM Tris-HCl, 100 U/l heparin, pH 7.4) and then sonicated three times in ice-cold water for 10 seconds with 30 second rests in between. To eliminate cell debris, the sample was centrifuged and the supernatant was used as reaction sample for spectrometric analysis, as previously described (Tiranti et al., 1995).

BN-PAGE analysis was basically performed as previously reported (Calvaruso et al., 2008) with small changes. Briefly, 1×10^7 cells were resuspended in 3× gel buffer (750 mM aminocaproic acid, 150 mM Bis-Tris pH 7.0) and the amount of protein quantified with the Bradford assay. N-dodecyl β-D-maltoside (Sigma) was added to a ratio 20 µg per µg total protein and made up to 40 µl with 3× gel buffer. 40 µg were loaded per lane for the CI detection, whereas 10 µg were loaded for MidA detection. For western blot analysis, the gel was transferred overnight at room temperature to a 0.45 µm PVDF membrane (PALL life sciences) at 30 V with 1× Tris-Gly, 20% methanol and 0.02% SDS buffer. Then, the membrane was stripped with 2% SDS, 62.5 mM Tris-HCl, pH 6.8, for 90 minutes. The western blot was carried out with total OXPHOS Human WB Antibody Cocktail (Mitosciences) to assay CI stability. A protein standard (Invitrogene) was used to estimate the size of the complexes. Secondary antibody goat anti-mouse IgG-HRP was provided by Santa Cruz Biotechnology. For MidA dimer experiments, the second dimension was made as previously described (Calvaruso et al., 2008). Anti-GFP (SIGMA) and goat anti-rabbit IgG-HRP (Santa Cruz) antibodies were used.

Site-directed mutagenesis
Site-directed mutagenesis of G170V and G172V was performed by PCR using as template the complete MidA gene cloned in pGEMt. Two complementary oligonucleotides containing the desired mutations were used. For G170V: oligo 1, CAA ATA GTT GAA ATG GTT CCA GGT AGA GGC ACA CTA ATG; oligo 2, CAT TAG TGT GCC TCT ACC TGG AAC CAT TTC AAC TAT TTG. For double mutation G170V and G172V: oligo 3, CAA ATA GTT GAA ATG GTT CCA GTT AGA GGC ACA CTA ATG. Oligo 4, CAT TAG TGT GCC TCT AAC TGG AAC CAT TTC AAC TAT TTG. The PCR reaction was digested with *Dpn*I and transformed into *E. coli* DH5α for plasmid amplification. The constructs were fully sequenced to confirm the mutations and cloned in-frame with GFP in the vector pDV-CGFP-CTAP, kindly provided by Pauline Shaap (University of Dundee, Dundee, UK). A similar construct was used with a complete wild-type sequence of MidA.

Pull-down assays
The N-terminus of *Dictyostelium* and human genes encoding NDUFS2 were expanded by PCR and cloned in PGEX plasmid (Pharmacia-Biotech) for bacterial expression and subsequent purification by the GST system according to the manufacturer's instructions. The *Dictyostelium* NDUFS2 construct spanned amino acids 8-176 and human NDUFS2 amino acids 38-234. GST alone was used as a control. The isolated proteins were kept associated with the Sepharose beads until used in the pull-down assay. 5×10^6 *Dictyostelium* and HEK293T cells expressing *Dictyostelium* or human MidA fused to GFP were resuspended in 500 µl STE+T buffer (10 mM Tris-HCl, pH 8, 1 mM EDTA pH 8, 150 mM NaCl, 5 mM DTT, 1% Triton X-100, 1× protease inhibitor cocktail) and shaken for 30 minutes at 4°C. After centrifugation, the supernatant was incubated with 30 µl of previously isolated proteins bound to the Sepharose beads for 1 hour at 4°C. Beads were washed three times with STE+T and finally resuspended in 30 µl protein loading buffer. The sample was split in two SDS-PAGE gels. One was stained with Coomassie Blue as a control and the other was transferred to PVDF for western blotting using anti-GFP antibody.

mtDNA and mtRNA quantification
For mtDNA quantification *Dictyostelium* cells were grown in HL-5 medium to log phase. Genomic DNA from 6×10^6 cells was extracted with 300 µl Quick Extract DNA Extraction Solution 1.0 (Epicentre). 1:50 dilution was used as a template in the PCR reaction carried out in 7900 HT Fast Real-Time PCR System, using Power Sybrgreen PCR Master Mix 2 with 300 nM oligonucleotides in a final volume of 10 µl. Results were acquired with SDS 2.3 software by Applied Biosystems and handled with Excel software by Microsoft. Two pairs of oligonucleotides were used: One for detection of mtDNA (DDB_G0294054), oligo1, AAC AAT CAT GTG GCT TTA GTA CGT AAA; oligo2, TCG GCC CTG CAT TTC GT and another for normalization with a nuclear gene (DDB_G0277273). Oligo 1, CCG TTG CCC TAA CTT ACT TCC A; oligo 2, GCC GCC ATT GAT GAA ACT ATT C. For mtRNA quantification, RNA from 1×10^7 cells growing to log phase in HL-5 medium was isolated with Tri-Reagent (Sigma) and adjusted to 2 µg/µl final concentration. DNA contamination was removed by adding 50 U DNase (New England Biolabs) to 10 µg RNA in a final volume of 10 µl. The reaction was incubated for 30 minutes at 37° C following an incubation at 70°C for 5 minutes to destroy DNase activity. The RNA was then adjusted with DEPC water to 100 ng/µl final concentration. 250 ng (2.5 µl) of this RNA was used as a template for RT-PCR with high capacity cDNA reverse transcription kit (Applied Biosystems) in a final volume of 20 µl. The cDNAs served as template in the PCR reaction carried out as described above. Eight genes

representative of the previously described eight major polycistronic transcripts (Barth et al., 2001) were studied for each sample, normalized to the nuclear gene DDB_G0277273 and referred to the wild-type levels. The oligonucleotides used are listed in supplementary material Table S2.

Phototaxis and thermotaxis assays

Qualitative phototaxis tests were performed as described (Darcy et al., 1994) by transferring a toothpick scraping of amoebae from a colony growing on a *K. aerogenes* lawn to the center of charcoal agar plates (5% activated charcoal, 1% agar). Phototaxis was scored after a 48 hour incubation at 21°C with a lateral light source. Quantitative phototaxis tests involved the harvesting of amoebae from mass plates, thoroughly washing them free of bacteria, suspending them in saline at the appropriate dilutions and inoculating 20 μl onto a 1 cm^2 area in the center of each charcoal agar plate. The resulting cell densities ranged from about $1.5×10^6$ to $3.7×10^7$ cells/cm^2. The phototaxis was again scored after a 48 hour incubation at 21°C with a lateral light source. Quantitative thermotaxis used washed amoebae prepared as for quantitative phototaxis and plated at a density of $3×10^6$ amoebae/cm^2. A 20 μl aliquot of cells at this dilution was plated on a 1 cm^2 area in the center of water agar plates (1% agar) and incubated for 72 hours in darkness on a heat bar producing a 0.2°C/cm gradient at the agar surface. The arbitrary temperature units correspond to the temperatures 14°C at T1 and increasing in 2°C increments to 28°C at T8, as measured at the center of plates in separate calibration experiments. Slug trails were transferred to PVC discs, stained with Coomassie blue and digitized. The orientation of the slug migration was analysed using directional statistics (Fisher, 1981).

Phagocytosis and pinocytosis assays

All *Dictyostelium* strains (wild type AX2, midA null mutant and the midA rescued strain) were grown in HL-5 medium with no antibiotics to exponential phase before use in the pinocytosis and phagocytosis experiments. Bacterial uptake by *Dictyostelium* strains was determined by using as prey an *E. coli* strain expressing fluorescent protein DsRed (Maselli et al., 2002) as previously described (Bokko et al., 2007).

Pinocytosis assays (Klein and Satre, 1986) were performed by measuring the uptake of medium containing a fluorescent indicator, fluorescein isothiocyanate (FITC)-dextran (Sigma, average mol. mass 70 kDa), as previously described (Bokko et al., 2007).

Supplementary material available online at
http://jcs.biologists.org/cgi/content/full/123/10/1674/DC1

References

Agrimi, G., Di Noia, M. A., Marobbio, C. M., Fiermonte, G., Lasorsa, F. M. and Palmieri, F. (2004). Identification of the human mitochondrial S-adenosylmethionine transporter: bacterial expression, reconstitution, functional characterization and tissue distribution. *Biochem. J.* **379**, 183-190.

Altschul, S. F., Madden, T. L., Schaffer, A. A., Zhang, J., Zhang, Z., Miller, W. and Lipman, D. J. (1997). Gapped BLAST and PSI-BLAST: a new generation of protein database search programs. *Nucleic Acids Res.* **25**, 3389-3402.

Andreeva, A., Howorth, D., Chandonia, J. M., Brenner, S. E., Hubbard, T. J., Chothia, C. and Murzin, A. G. (2008). Data growth and its impact on the SCOP database: new developments. *Nucleic Acids Res.* **36**, D419-D425.

Annesley, S. J. and Fisher, P. R. (2009a). *Dictyostelium discoideum*-a model for many reasons. *Mol. Cell Biochem.* **329**, 73-91.

Annesley, S. J. and Fisher, P. R. (2009b). *Dictyostelium* slug phototaxis. *Methods Mol. Biol.* **571**, 67-76.

Barth, C., Greferath, U., Kotsifas, M., Tanaka, Y., Alexander, S., Alexander, H. and Fisher, P. R. (2001). Transcript mapping and processing of mitochondrial RNA in *Dictyostelium discoideum*. *Curr. Genet.* **39**, 355-364.

Barth, C., Le P. and Fisher, P. R. (2007). Mitochondrial biology and disease in *Dictyostelium*. *Int. Rev. Cytol.* **263**, 207-252.

Bokko, P. B., Francione, L., Bandala-Sanchez, E., Ahmed, A. U., Annesley, S. J., Huang, X., Khurana, T., Kimmel, A. R. and Fisher, P. R. (2007). Diverse cytopathologies in mitochondrial disease are caused by AMP-activated protein kinase signaling. *Mol. Biol. Cell* **18**, 1874-1886.

Bych, K., Kerscher, S., Netz, D. J., Pierik, A. J., Zwicker, K., Huynen, M. A., Lill, R., Brandt, U. and Balk, J. (2008). The iron-sulphur protein Ind1 is required for effective complex I assembly. *EMBO J.* **27**, 1736-1746.

Calvaruso, M. A., Smeitink, J. and Nijtmans, L. (2008). Electrophoresis techniques to investigate defects in oxidative phosphorylation. *Methods* **46**, 281-287.

Carroll, J., Fearnley, I. M., Skehel, J. M., Runswick, M. J., Shannon, R. J., Hirst, J. and Walker, J. E. (2005). The post-translational modifications of the nuclear encoded subunits of complex I from bovine heart mitochondria. *Mol. Cell Proteomics* **4**, 693-699.

Chida, J., Yamaguchi, H., Amagai, A. and Maeda, Y. (2004). The necessity of mitochondrial genome DNA for normal development of *Dictyostelium* cells. *J. Cell Sci.* **117**, 3141-3152.

Darcy, P. K., Wilczynska, Z. and Fisher, P. R. (1994). Genetic analysis of *Dictyostelium* slug phototaxis mutants. *Genetics* **137**, 977-985.

Debray, F. G., Lambert, M. and Mitchell, G. A. (2008). Disorders of mitochondrial function. *Curr. Opin. Pediatr.* **20**, 471-482.

DiMauro, S. and Schon, E. A. (2008). Mitochondrial disorders in the nervous system. *Annu. Rev. Neurosci.* **31**, 91-123.

Eichinger, L., Pachebat, J. A., Glockner, G., Rajandream, M. A., Sucgang, R., Berriman, M., Song, J., Olsen, R., Szafranski, K., Xu, Q. et al. (2005). The genome of the social amoeba *Dictyostelium discoideum*. *Nature* **435**, 43-57.

Escalante, R. and Vicente, J. J. (2000). *Dictyostelium discoideum*: a model system for differentiation and patterning. *Int. J. Dev. Biol.* **44**, 819-835.

Fearnley, I. M., Carroll, J. and Walker, J. E. (2007). Proteomic analysis of the subunit composition of complex I (NADH:ubiquinone oxidoreductase) from bovine heart mitochondria. *Methods. Mol. Biol.* **357**, 103-125.

Finn, R. D., Tate, J., Mistry, J., Coggill, P. C., Sammut, S. J., Hotz, H. R., Ceric, G., Forslund, K., Eddy, S. R., Sonnhammer, E. L. et al. (2008). The Pfam protein families database. *Nucleic Acids Res.* **36**, D281-D288.

Fisher, P. R., Smith, E. and Williams, K. L. (1981). An extracellular chemical signal controlling phototactic behavior by *D. discoideum* slugs. *Cell* **23**, 799-807.

Gerards, M., Sluiter, W., van den Bosch, B. J., de Wit, E., Calis, C. M., Frentzen, M., Akbari, H., Schoonderwoerd, K., Scholte, H. R., Jongbloed, R. J. et al. (2009). Defective complex I assembly due to C20orf7 mutations as a new cause of Leigh syndrome. *J. Med. Genet.* PMID: 19452079.

Helm, M., Brule, H., Degoul, F., Cepanec, C., Leroux, J. P., Giege, R. and Florentz, C. (1998). The presence of modified nucleotides is required for cloverleaf folding of a human mitochondrial tRNA. *Nucleic Acids Res.* **26**, 1636-1643.

Hoefs, S. J., Dieteren, C. E., Rodenburg, R. J., Naess, K., Bruhn, H., Wibom, R., Wagena, E., Willems, P. H., Smeitink, J. A., Nijtmans, L. G. et al. (2009). Baculovirus complementation restores a novel NDUFAF2 mutation causing complex I deficiency. *Hum. Mutat.* **30**, E728-E736.

Janssen, R. J., Nijtmans, L. G., van den Heuvel, L. P. and Smeitink, J. A. (2006). Mitochondrial complex I: structure, function and pathology. *J. Inherit. Metab. Dis.* **29**, 499-515.

Kagan, R. M. and Clarke, S. (1994). Widespread occurrence of three sequence motifs in diverse S-adenosylmethionine-dependent methyltransferases suggests a common structure for these enzymes. *Arch. Biochem. Biophys.* **310**, 417-427.

Kakebeeke, P. I. J., de Wit, R. J. W., Kohtz, S. D. and Konijn, T. M. (1979). Negative chemotaxis in *Dictyostelium* and *Polysphondylium*. *Exp. Cell Res.* **124**, 429-433.

Kelley, L. A. and Sternberg, M. J. (2009). Protein structure prediction on the Web: a case study using the Phyre server. *Nat. Protoc.* **4**, 363-371.

Kirchmair, J., Markt, P., Distinto, S., Schuster, D., Spitzer, G. M., Liedl, K. R., Langer, T. and Wolber, G. (2008). The Protein Data Bank (PDB), its related services and software tools as key components for in silico guided drug discovery. *J. Med. Chem.* **51**, 7021-7040.

Klein, G. and Satre, M. (1986). Kinetics of fluid-phase pinocytosis in *Dictyostelium discoideum* amoebae. *Biochem. Biophys. Res. Commun.* **138**, 1146-1152.

Koopman, W. J., Nijtmans, L. G., Dieteren, C. E., Roestenberg, P., Valsecchi, F., Smeitink, J. A. and Willems, P. H. (2010). Mammalian mitochondrial complex I: biogenesis, regulation and reactive oxygen species generation. *Antioxid. Redox Signal.* PMID: 19803744.

Kotsifas, M., Barth, C., De Lozanne, A., Lay, S. T. and Fisher, P. R. (2002). Chaperonin 60 and mitochondrial disease in *Dictyostelium*. *J. Muscle Res. Cell Motil.* **23**, 839-852.

Lazarou, M., Thorburn, D. R., Ryan, M. T. and McKenzie, M. (2009). Assembly of mitochondrial complex I and defects in disease. *Biochim. Biophys. Acta.* **1793**, 78-88.

Loeffen, J., Elpeleg, O., Smeitink, J., Smeets, R., Stockler-Ipsiroglu, S., Mandel, H., Sengers, R., Trijbels, F. and van den Heuvel, L. (2001). Mutations in the complex I NDUFS2 gene of patients with cardiomyopathy and encephalomyopathy. *Ann. Neurol.* **49**, 195-201.

Loenen, W. A. (2006). S-adenosylmethionine: jack of all trades and master of everything? *Biochem. Soc. Trans.* **34**, 330-333.

Lopez, G., Valencia, A. and Tress, M. L. (2007). firestar-prediction of functionally important residues using structural templates and alignment reliability. *Nucleic Acids Res.* **35**, W573-W577.

Martin, J. L. and McMillan, F. M. (2002). SAM (dependent) I AM: the S-adenosylmethionine-dependent methyltransferase fold. *Curr. Opin. Struct. Biol.* **12**, 783-793.

Maselli, A., Laevsky, G. and Knecht, D. A. (2002). Kinetics of binding, uptake and degradation of live fluorescent (DsRed) bacteria by *Dictyostelium discoideum*. *Microbiology* **148**, 413-420.

Niewmierzycka, A. and Clarke, S. (1999). S-Adenosylmethionine-dependent methylation in *Saccharomyces cerevisiae*. Identification of a novel protein arginine methyltransferase. *J. Biol. Chem.* **274**, 814-824.

Ogawa, S., Yoshino, R., Angata, K., Iwamoto, M., Pi, M., Kuroe, K., Matsuo, K., Morio, T., Urushihara, H., Yanagisawa, K. et al. (2000). The mitochondrial DNA of *Dictyostelium discoideum*: complete sequence, gene content and genome organization. *Mol. Gen. Genet.* **263**, 514-519.

Ogilvie, I., Kennaway, N. G. and Shoubridge, E. A. (2005). A molecular chaperone for mitochondrial complex I assembly is mutated in a progressive encephalopathy. *J. Clin. Invest.* **115**, 2784-2792.

Pagliarini, D. J., Calvo, S. E., Chang, B., Sheth, S. A., Vafai, S. B., Ong, S. E., Walford, G. A., Sugiana, C., Boneh, A., Chen, W. K. et al. (2008). A mitochondrial protein compendium elucidates complex I disease biology. *Cell* **134**, 112-123.

Pang, K. M., Lynes, M. A. and Knecht, D. A. (1999). Variables controlling the expression level of exogenous genes in *Dictyostelium*. *Plasmid* **41**, 187-197.

Pathak, R. U. and Davey, G. P. (2008). Complex I and energy thresholds in the brain. *Biochim. Biophys. Acta* **1777**, 777-782.

Pintard, L., Bujnicki, J. M., Lapeyre, B. and Bonnerot, C. (2002). MRM2 encodes a novel yeast mitochondrial 21S rRNA methyltransferase. *EMBO J.* **21**, 1139-1147.

Porter, C. T., Bartlett, G. J. and Thornton, J. M. (2004). The Catalytic Site Atlas: a resource of catalytic sites and residues identified in enzymes using structural data. *Nucleic Acids Res.* **32**, D129-D133.

Rain, J. C., Selig, L., De Reuse, H., Battaglia, V., Reverdy, C., Simon, S., Lenzen, G., Petel, F., Wojcik, J., Schachter, V. et al. (2001). The protein-protein interaction map of *Helicobacter pylori*. *Nature* **409**, 211-215.

Remacle, C., Barbieri, M. R., Cardol, P. and Hamel, P. P. (2008). Eukaryotic complex I: functional diversity and experimental systems to unravel the assembly process. *Mol. Genet. Genomics* **280**, 93-110.

Saada, A., Vogel, R. O., Hoefs, S. J., van den Brand, M. A., Wessels, H. J., Willems, P. H., Venselaar, H., Shaag, A., Barghuti, F., Reish, O. et al. (2009). Mutations in NDUFAF3 (C3ORF60), encoding an NDUFAF4 (C6ORF66)-interacting complex I assembly protein, cause fatal neonatal mitochondrial disease. *Am. J. Hum. Genet.* **84**, 718-727.

Sadreyev, R. I., Baker, D. and Grishin, N. V. (2003). Profile-profile comparisons by COMPASS predict intricate homologies between protein families. *Protein Sci.* **12**, 2262-2272.

Schubert, H. L., Blumenthal, R. M. and Cheng, X. (2003). Many paths to methyltransfer: a chronicle of convergence. *Trends Biochem. Sci.* **28**, 329-335.

Shaulsky, G. and Loomis, W. F. (1993). Cell type regulation in response to expression of ricin-A in *Dictyostelium*. *Dev. Biol.* **160**, 85-98.

Sugiana, C., Pagliarini, D. J., McKenzie, M., Kirby, D. M., Salemi, R., Abu-Amero, K. K., Dahl, H. H., Hutchison, W. M., Vascotto, K. A., Smith, S. M. et al. (2008). Mutation of C20orf7 disrupts complex I assembly and causes lethal neonatal mitochondrial disease. *Am. J. Hum. Genet.* **83**, 468-478.

Sussman, M. (1987). Cultivation and synchronous morphogenesis of *Dictyostelium* under controlled experimental conditions. *Meth. Cell Biol.* **28**, 9-29.

Tiranti, V., Chariot, P., Carella, F., Toscano, A., Soliveri, P., Girlanda, P., Carrara, F., Fratta, G. M., Reid, F. M., Mariotti, C. et al. (1995). Maternally inherited hearing loss, ataxia and myoclonus associated with a novel point mutation in mitochondrial tRNASer(UCN) gene. *Hum. Mol. Genet.* **4**, 1421-1427.

Torija, P., Robles, A. and Escalante, R. (2006a). Optimization of a large-scale gene disruption protocol in *Dictyostelium* and analysis of conserved genes of unknown function. *BMC Microbiol.* **6**, 75.

Torija, P., Vicente, J. J., Rodrigues, T. B., Robles, A., Cerdan, S., Sastre, L., Calvo, R. M. and Escalante, R. (2006b). Functional genomics in *Dictyostelium*: MidA, a new conserved protein, is required for mitochondrial function and development. *J. Cell Sci.* **119**, 1154-1164.

Ugalde, C., Janssen, R. J., van den Heuvel, L. P., Smeitink, J. A. and Nijtmans, L. G. (2004). Differences in assembly or stability of complex I and other mitochondrial OXPHOS complexes in inherited complex I deficiency. *Hum. Mol. Genet.* **13**, 659-667.

Vahsen, N., Cande, C., Briere, J. J., Benit, P., Joza, N., Larochette, N., Mastroberardino, P. G., Pequignot, M. O., Casares, N., Lazar, V. et al. (2004). AIF deficiency compromises oxidative phosphorylation. *EMBO J.* **23**, 4679-4689.

Vogel, R. O., Janssen, R. J., Ugalde, C., Grovenstein, M., Huijbens, R. J., Visch, H. J., van den Heuvel, L. P., Willems, P. H., Zeviani, M., Smeitink, J. A. et al. (2005). Human mitochondrial complex I assembly is mediated by NDUFAF1. *FEBS J.* **272**, 5317-5326.

Vogel, R. O., Janssen, R. J., van den Brand, M. A., Dieteren, C. E., Verkaart, S., Koopman, W. J., Willems, P. H., Pluk, W., van den Heuvel, L. P., Smeitink, J. A. et al. (2007). Cytosolic signaling protein Ecsit also localizes to mitochondria where it interacts with chaperone NDUFAF1 and functions in complex I assembly. *Genes Dev.* **21**, 615-624.

Wallace, A. C., Laskowski, R. A. and Thornton, J. M. (1995). LIGPLOT: a program to generate schematic diagrams of protein-ligand interactions. *Prot. Eng.* **8**, 127-134.

Wilczynska, Z., Barth, C. and Fisher, P. R. (1997). Mitochondrial mutations impair signal transduction in *Dictyostelium discoideum* slugs. *Biochem. Biophys. Res. Commun.* **234**, 39-43.

Williams, R. S., Boeckeler, K., Graf, R., Muller-Taubenberger, A., Li, Z., Isberg, R. R., Wessels, D., Soll, D. R., Alexander, H. and Alexander, S. (2006). Towards a molecular understanding of human diseases using *Dictyostelium discoideum*. *Trends Mol. Med.* **12**, 415-424.

Wu, C. C., MacCoss, M. J., Howell, K. E. and Yates, J. R., 3rd. (2003). A method for the comprehensive proteomic analysis of membrane proteins. *Nat. Biotechnol.* **21**, 532-538.

Zemla, A. (2003). LGA: a method for finding 3D similarities in protein structures. *Nucleic Acids Res.* **31**, 3370-3374.